

Original Paper

# miR-137 Inhibits Proliferation and Metastasis of Hypertrophic Scar Fibroblasts via Targeting Pleiotrophin

Qian Zhang Bingyu Guo Qiang Hui Peng Chang Kai Tao

Reconstructive and Plastic Surgery, The General Hospital of Shenyang Military Region, Shenyang, China

## Key Words

Ptn • Hypertrophic scar • miR-137 • Proliferation • Metastasis

## Abstract

**Background/Aims:** There are few effective treatment options for hypertrophic scars. MicroRNAs are a class of small, noncoding RNAs involved in multiple biological functions. **Methods:** Gene chip screening was used to screen out the differential expression of miRNAs in hypertrophic scars and normal tissues. Western blot and real-time PCR were used to confirm the expression of pleiotrophin (PTN) in hypertrophic scars. After analyze the correlation between PTN and miR-137 using correlation analysis, we used miRDB software to analyze the binding sites of miR-137 and PTN. Luciferase reporter gene, western blot and real-time PCR experiments were used to detect the regulatory effect of miR-137 on PTN. MTT and transwell assay were used to detect the effect of miR-137 on proliferation and metastasis. Western blot and real-time PCR were used to detect the regulatory effects of miR-137 on cyclin B1, matrix metalloproteinase 9 (MMP9),  $\alpha$ -smooth muscle actin ( $\alpha$ -SMA), vimentin, and type-I collagen (COL1A). Finally, miR-137 inhibitor was transfected into fibroblasts which was silent PTN, and the proliferation and migration of cells were detected by MTT and transwell. Western blot and real-time PCR were used to detect the expression of related proteins. **Results:** Various miRNAs was abnormal expressed in hypertrophic scars. miR-137 was decreased in hypertrophic scar, however PTN was up regulated in hypertrophic scars. miR-137 induced proliferation and metastasis in fibroblasts. This effect was accompanied by decreased expression of cyclin B1, MMP9,  $\alpha$ -SMA, vimentin, and COL1A mediated via the target of PTN. **Conclusion:** Modulation of miR-137 expression in fibroblasts could provide an important therapeutic strategy for hypertrophic scars.

© 2018 The Author(s)  
Published by S. Karger AG, Basel

Q. Zhang and B. Guo contributed equally to this work.

Peng Chang  
and Kai Tao

Reconstructive and Plastic Surgery, The General Hospital of Shenyang Military Region  
83#Wenhua Road, Shenhe District, Shenyang, Liaoning, 110016 (China)  
Tel. +86-24-28851313, E-Mail cp17625@163.com; luzongzhengxing@sina.com

## Introduction

Hypertrophic scar and keloid are two types of pathological scar [1]. Patients with hypertrophic scars experience physical pain and stress, such as itching and skin contraction, as well as psychological distress. In addition to surgery, current treatments for hypertrophic scars mainly include glucocorticoid injection, silicone membrane therapy, compression therapy, cryotherapy, laser therapy, radiotherapy, and interferon growth factor therapy [2]. Each type of therapy usually requires multiple treatments and has some limitations. Thus, more convenient, effective, and safe methods for the treatment of hypertrophic scars are needed [3, 4].

Increasing evidence implicates microRNAs (miRNAs) as important regulatory factors in tumorigenesis and hypertrophic scars, and they are found to be dysregulated in the majority of analyzed cancers and pathological scars [5-7].

Pleiotrophin (PTN) is a secreted, heparin-binding growth factor that has a role in various biological functions such as cell growth, differentiation, and tumor progression. PTN expression was reported to be increased in hypertrophic scars [8].

In this study, we demonstrated that miR-137 induced proliferation, metastasis and differentiation in fibroblasts. This effect was accompanied by decreased expression of cyclin B1, matrix metalloproteinase 9 (MMP9),  $\alpha$ -smooth muscle actin ( $\alpha$ -SMA), vimentin, and type-I collagen (COL1A) mediated via the PTN pathway. These results suggest that modulation of miR-137 expression in fibroblasts could provide an important therapeutic strategy for hypertrophic scars and warrants further investigation.

## Materials and Methods

### *Tissue samples and cell lines*

Tissue samples of hypertrophic scar and paired normal tissue obtained as excess from partial skin flaps. Samples were obtained from 30 patients during plastic surgery. Patients were admitted to the Reconstructive and Plastic Surgery Department of General Hospital of Shenyang Military Region from May 2012 to May 2016. Before surgery, written informed consent was obtained from all participants. The protocols were approved by the Ethics Committee of General Hospital of Shenyang Military Command.

Healthy skin and hypertrophic scar tissues were minced, and epidermal and dermal layers were separated by treatment with dispase II (Life Technologies, Carlsbad, CA) for the isolation of primary human skin fibroblasts and hypertrophic scar fibroblasts. Tissue was digested with collagenase type I (Sigma-Aldrich, St. Louis, MO). Fibroblasts were harvested and grown in Dulbecco's modified Eagle's medium (DMEM) supplemented with 10% fetal bovine serum (Hyclone Technologies, Logan, UT), at 37 °C in 5% CO<sub>2</sub>. Fibroblasts at passages 2-5 were used for all experiments in this study [9].

### *RNA isolation*

Total RNAs were extracted from tissues and cells using miRcute miRNA Isolation Kit (Tiangen Biotech (Beijing) Co., Ltd., Beijing, China) according to the manufacturer's instruction. Samples were stored at -80°C.

### *miRNA microarray analysis*

A total of 500 ng RNA was subjected to Agilent miRNA microarray analysis (RiboBio, Beijing, China). Differences between groups were examined for statistical significance using unpaired Student's t-test.

### *Real-time PCR*

Real-time PCR was performed using Real-time PCR Universal Reagent and the MX3000P Real-time PCR instrument following the manufacturer's protocols (Suobao, Shanghai, China). U6 small nuclear RNA was used as an internal control. The expression of miR-137 was detected using the Stem-Loop RT-PCR assay as previously reported [10, 11]. Primer sequences are listed in Table 1.

All reactions were carried out as described previously [12].

### Western blot analyses

Cells and tissues were lysed and protein was extracted using lysis buffer. Lysate was prepared using NP40 buffer supplemented with proteinase inhibitor cocktail. Samples were resolved by 10% sodium dodecyl sulfate polyacrylamide gel electrophoresis and transferred onto polyvinylidene fluoride (PVDF) membranes. PVDF membranes were blocked with phosphate-buffered saline containing 2% bovine serum albumin and 0.05% Tween-20 overnight at 4°C. Membranes were then probed with primary antibodies for 1 h at room temperature. Next, membranes were washed and incubated with goat-anti-mouse secondary antibody for 1 h at room temperature. Expression levels of relevant proteins were quantified and normalized relative to GAPDH. Antibodies used for western blotting were: anti-PTN (1:300), anti-cyclin B1 (1:500), anti-MMP9 (1:500), anti- $\alpha$ -smooth muscle actin ( $\alpha$ -SMA) (1:300), anti-vimentin (1:500), anti-type-I collagen (COL1A; 1:500), and anti-GAPDH (1:1000), and horseradish peroxidase-conjugated anti-mouse (1:5000) and anti-rabbit (1:5000) secondary antibodies (Santa Cruz Biotechnology, Santa Cruz, CA).

### Dual luciferase reporter assay

Dual luciferase activity assays were performed as previously described [13]. The PTN 3' untranslated region (3'-UTR) was PCR amplified and cloned into the pMiR-REPORT™ vector (Ambion, Shanghai, China). The primers were: PTN-WT, F: 5'- CAATTCCCGTCCCTCCAAA -3', R: 5'- TGTGCATGACATCCAACCTGAA -3', PTN-mut (the site of miR-137 binding was mutated), F: 5'- CCCCGTCCCTCCAAAATCTC -3', R: 5'- TTGTGCATGACATCCAACCTGA -3'. Cells were seeded and co-transfected with the above constructs and miR-137 mimic (RiboBio), miR-137 antisense (RiboBio) or control (RiboBio). After 24 h, fibroblasts were harvested and luciferase activity was analyzed using the Dual-Luciferase Reporter Assay System (Biotek Synergy, Beijing, China).

### MTT assay

Cell proliferation was measured using the MTT assay (Solarbio, Beijing, China). Cells were seeded at a density of  $1 \times 10^3$  cells per well in 96-well plates, and transfected with miR-137 mimic, miR-137 inhibitor (RiboBio), or negative control; then, cell proliferation was evaluated by MTT assay. A microplate reader (Bio-Rad Laboratories, Hercules, CA) was used to measure optical density at 490 nm.

### Transwell migration assay

Twenty-four hours after transfection with miR-137 mimic, miR-137 inhibitor, or negative control,  $1 \times 10^5$  cells in serum-free medium were seeded in transwell chambers with or without a Matrigel cover. and the transwell migration assay was performed. After 8 h, cells were fixed with 4% paraformaldehyde and stained with 0.4% trypan blue.

### Measurement of contraction rate of fibroblast collagen network

Control, miR-137 mimic, or miR-137 inhibitor was transfected into human skin fibroblasts and hypertrophic scar fibroblasts. After transfection for 24 h,  $2 \times 10^4$  cells were mixed with 100  $\mu$ L collagen solution (Boosen, Beijing, China) with 300  $\mu$ L 10  $\times$  DMEM. After mixing, the cells were incubated at 37°C for 10

**Table 1.** Primer sequences

Name	Forward primer (5'→3')	Reverse primer (5'→3')
Hsa-miR-137	ACACTCATTATTGCTTA	CTACGCGTATTGAGAGTAC
Hsa-miR-627-3p	CACTCATCTTTTCTTTG	GAGTCTCTTGAGAGTACAT
Hsa-miR-219b-5p	ACTCAAGATGTCCAGCC	CGAAGATTGTTGAGAGTAC
Hsa-miR-96-3p	CACTCTAAATCATGTGC	CATATTGGCCCTTGAGAGTA
Hsa-miR-548c-3p	CACTCTAGAAAAATCTC	GCAAAAAGTTTGAGAGTACA
Hsa-miR-384	ACACTCTAATTCCTAGA	TATGAACTTGAGAGTACAT
Hsa-miR-670-3p	ACACTCTATTCTCTCAT	TCCTGAATGTTGAGAGTAC
Hsa-miR-5692b	ACACTCTAATAATATC	ACACCTACTTGAGAGTACA
Hsa-miR-190a-3p	ACTCTACTATATATCAA	AGGAATATGTTGAGAGTAC
U6	CTCGCTTCGGCAGCACA	ACGCTTCACGAATTTGC
PTN	CCATTTCCCTTCGGTTCC	AGGTTGCCTACCGCTGAGTCC
Cyclin B1	CAGTCAGACCAAATACTACTGCG	CACCAACCAGCTGCAGCATCTTC
MMP9	CCTGGAGACCTGAGAACCAATC	CCACCCGAGTGAACCATAGC
$\alpha$ -SMA	GGTACCACCATGTACCAGG	CCAGGGCTACAGTTAAGGG
Vimentin	GGACCAGCTAACCAACGACA	AAGGTCAAGACGTGCCAGAG
COL1A	GGTCCCCTGGAAGAATGG	GGACCTTCAGACCTCGGG
GAPDH	CATCCCTTCTCCACAC	GTCCAGGGCTTGTATTG

**Table 2.** Differential miRNA expression in hypertrophic scars

miRNA	P values	Fold change (hypertrophic scar/adjacent tissues)	Trend
Hsa-miR-137	8.52E-06	71.253	down
Hsa-miR-627-3p	7.19E-05	64.209	down
Hsa-miR-219b-5p	5.31E-05	62.192	down
Hsa-miR-96-3p	0.001	58.321	down
Hsa-miR-548c-3p	0.009	54.291	down
Hsa-miR-384	0.012	36.887	down
Hsa-miR-670-3p	0.018	30.176	down
Hsa-miR-5691	0.021	12.375	down
Hsa-miR-3193-3p	0.027	9.903	down
Hsa-miR-6805-3p	0.034	3.186	down
Hsa-miR-5692b	6.77E-06	42.763	Up
Hsa-miR-190a-3p	5.24E-05	36.578	Up
Hsa-miR-513a-3p	8.09E-04	21.904	Up
Hsa-miR-1279	0.001	17.653	Up
Hsa-miR-514b-3p	0.001	12.145	Up
Hsa-miR-19a-3p	0.031	8.372	Up
Hsa-miR-29b-3p	0.038	3.094	Up
Hsa-miR-3974	0.043	1.283	Up

min, then 2 mL DMEM was added. After the gel was separated from the bottom wall of the culture dish, the culture was maintained at 37°C. The gel diameter was measured at 0, 24, and 48 h, and the shrinkage index of the gel block was calculated.

#### Statistical analysis

All data were analyzed with SPSS 17.0 (SPSS Inc., Chicago, IL). Statistical significance was defined as  $P < 0.05$ . All experiments were repeated three times.

## Results

### Differential expression profile of miRNAs in hypertrophic scar tissues

The miRNA microarray showed 10 underexpressed miRNAs ( $P < 0.05$ ) and 8 overexpressed miRNAs ( $P < 0.05$ ) in hypertrophic scar tissues compared with the adjacent normal tissues (Table 2). Among these 18 miRNAs, we found a fold change of  $>30$  in 9 miRNAs, with the largest fold change (71.253) for miR-137. The expressions of these miRNAs in hypertrophic scar tissues and adjacent normal tissues were detected by real-time PCR (Fig. 1A). The results showed that miR-137 decreased significantly in hypertrophic scar tissues.

### The expression of PTN in hypertrophic scar tissues

Using MiRDB software, we showed that miR-137 can target multiple proteins. Among them PTN, a previously identified protein overexpressed in hypertrophic scars, has been shown to bind to miR-137. The expression of PTN in hypertrophic scar tissues and adjacent tissues was detected by western blotting and real-time PCR (Fig. 1 B, C). Results showed that there was a higher expression of PTN in hypertrophic scar tissues than the adjacent tissues.

### Relationship between miR-137 and PTN in hypertrophic scar fibroblasts

Using correlation analysis, we found a negative association between the expressions of miR-137 and PTN in hypertrophic scars (Fig. 2A). We also found that miR-137 could be combined

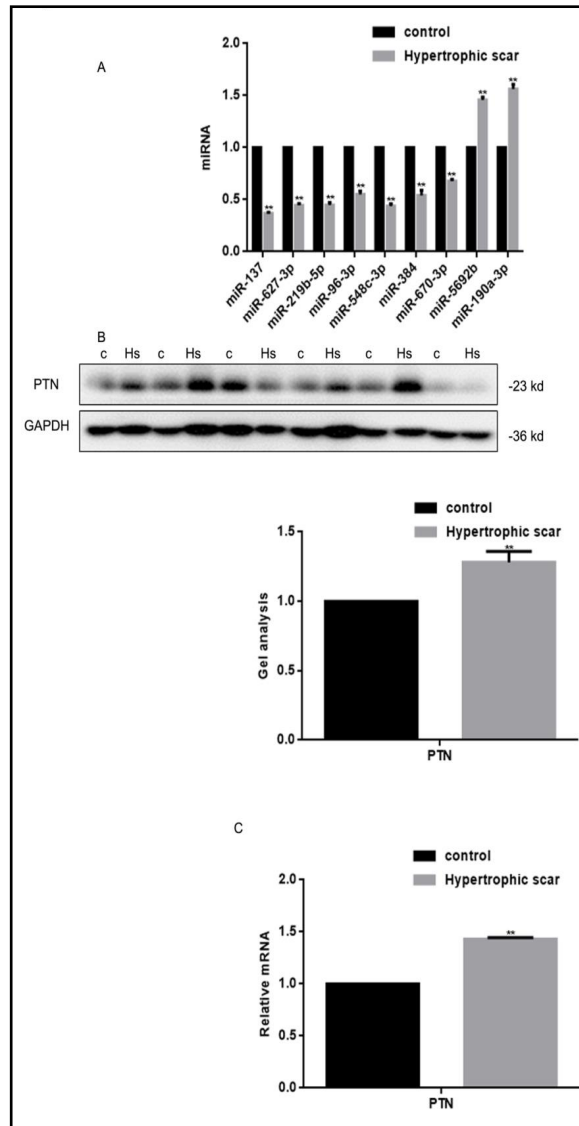


**Fig. 1.** Expression of miRNAs and PTN in hypertrophic scar tissues. (A) Expression of miRNAs in hypertrophic scar tissues and adjacent tissues were detected by real-time PCR. \*\*  $P < 0.01$  vs. adjacent tissues. (B) Protein levels of PTN in hypertrophic scar tissues and adjacent tissues were detected with western blotting. The expression of PTN was higher in hypertrophic scar tissues. Data are presented as the mean  $\pm$  standard error of the mean (SEM). \*\*  $P < 0.01$  vs. adjacent tissues. (C) mRNA expression levels of PTN in hypertrophic scar tissues and adjacent tissues were detected by real-time PCR. The expression of PTN was higher in the hypertrophic scar tissues. Data are presented as the mean  $\pm$  SEM. \*\*  $P < 0.01$  vs. adjacent tissues.

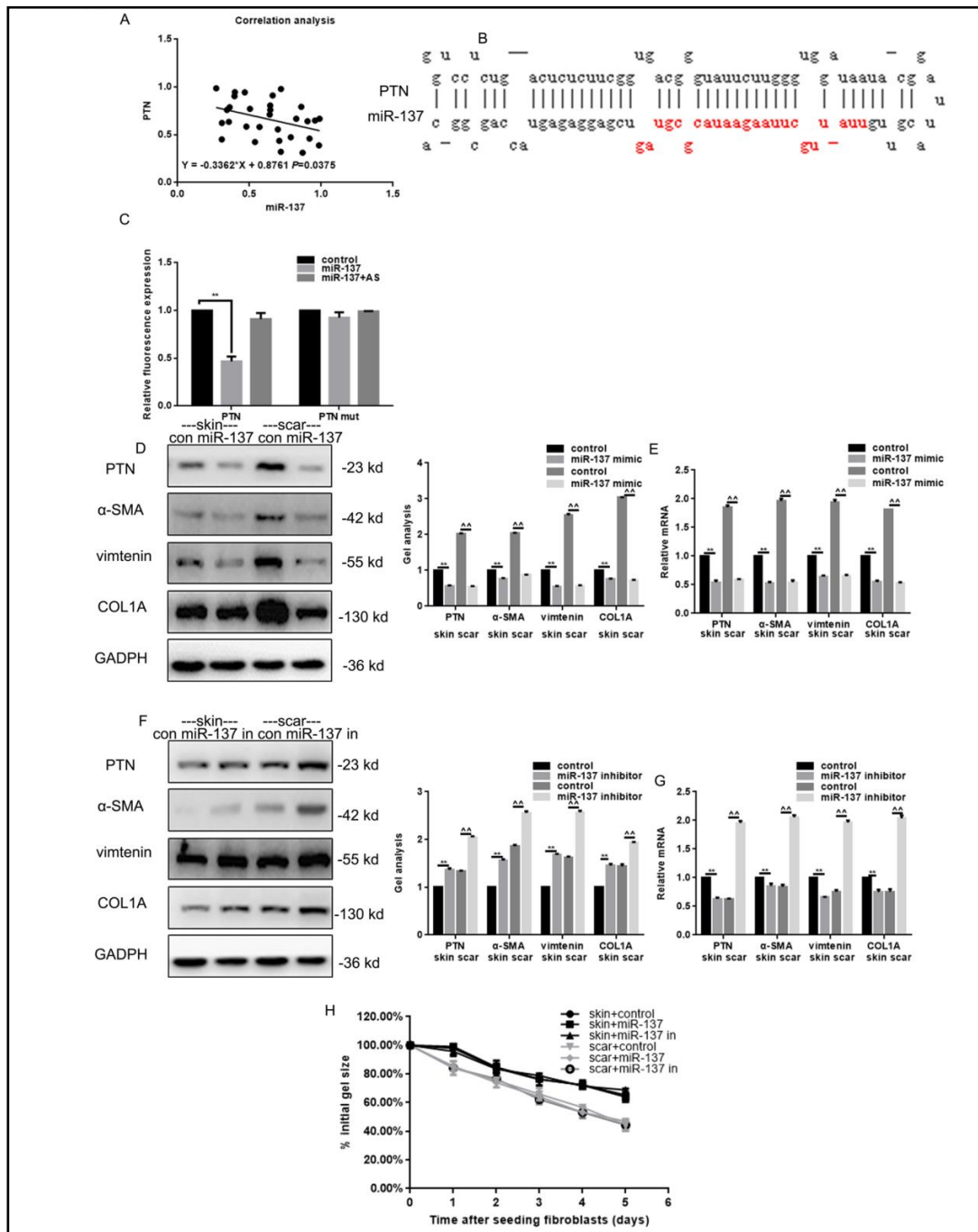
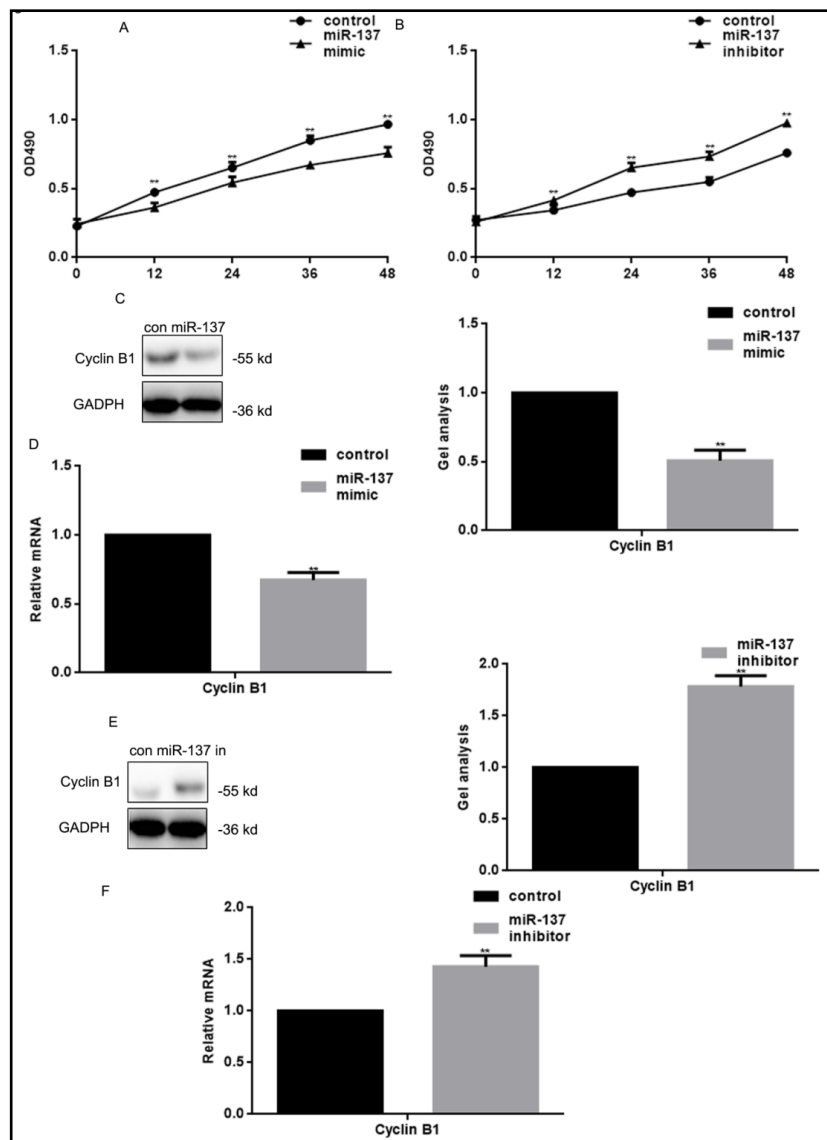


**Fig. 2.** Relationship between miR-137 and PTN. (A) Correlation between the expression levels of miR-137 and PTN in hypertrophic scars. (B) miRDB predicted that miR-137 could be combined specifically with PTN. (C) Interaction between miR-137 and the PTN 3'-UTR was tested by luciferase reporter assays. Data are presented as the mean  $\pm$  SEM. \*\*  $P < 0.01$  vs. control group. (D, E) Western blotting and real-time PCR showed that when the miR-137 was overexpressed, PTN,  $\alpha$ -SMA, vimentin and COL1A were downregulated in both skin fibroblasts and hypertrophic scar fibroblasts. Data are presented as the mean  $\pm$  SEM. \*\*  $P < 0.01$  vs. control group; ^^  $P < 0.01$  vs. control group. (F, G) Western blotting and real-time PCR showed that when miR-137 expression was decreased, PTN,  $\alpha$ -SMA, vimentin, and COL1A were upregulated in both skin fibroblasts and hypertrophic scar fibroblasts. Data are presented as the mean  $\pm$  SEM. \*\*  $P < 0.01$  vs. control group; ^^  $P < 0.01$  vs. control group. (H) Contraction of fibroblasts in the presence or absence of miR-137 or miR-137 inhibitor.

with 3'-UTR of PTN by miRDB (Fig. 2B). A luciferase reporter assay showed that miR-137 can reduce the expression of PTN at the transcriptional level in hypertrophic scar fibroblasts (Fig. 2C). When cells were co-transfected with PTN and miR-137, luciferase activity was reduced; however, luciferase activity did not vary significantly in the cells co-transfected with PTN mut or miR-137 antisense. Next, we transfected miR-137 mimic or miR-137 inhibitor into human skin fibroblasts and hypertrophic scar fibroblasts, and western blotting and real-time PCR showed that the expression levels of PTN,  $\alpha$ -SMA, vimentin, and COL1A were downregulated significantly by miR-137 (Fig. 2D-G). We also found that the collagen gel started to shrink within 1 day of seeding the hypertrophic scar fibroblasts, and the area gradually reached 40% of its initial size over the next 5 days. Transfection of miR-137 mimic/inhibitor in fibroblasts had minimal effect on the size of the gel over the 5 days (Fig. 2H).

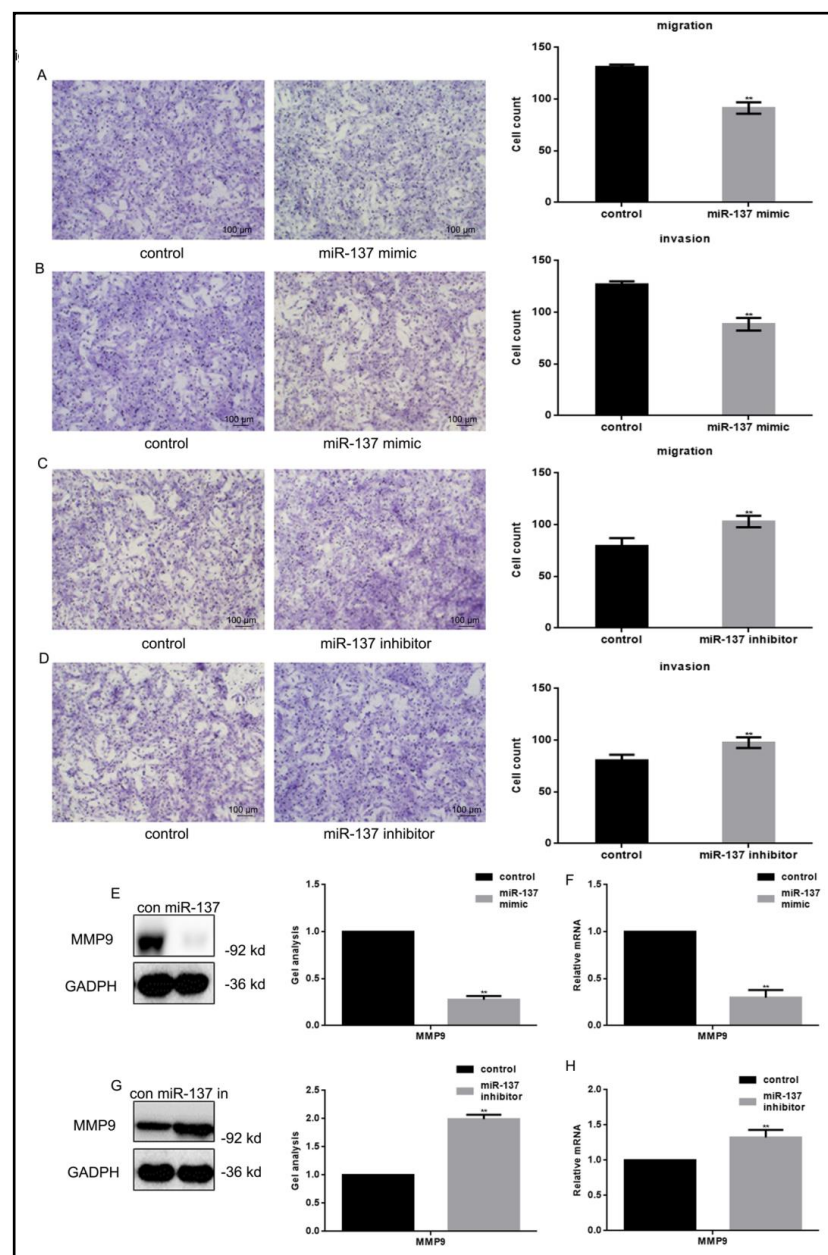
**Fig. 3.** miR-137 inhibits the proliferation of hypertrophic scar fibroblasts by suppressing cyclin B1. (A) MTT assay showed that proliferation of hypertrophic scar fibroblasts was repressed after transfection with miR-137 mimic. Data are presented as the mean  $\pm$  SEM. \*\*  $P < 0.01$  vs. control group. (B) MTT assay showed that proliferation of hypertrophic scar fibroblasts was promoted by transfection with miR-137 inhibitor. Data are presented as the mean  $\pm$  SEM. \*\*  $P < 0.01$  vs. control group. (C, D) After transfection with miR-137 mimic in hypertrophic scar fibroblasts, expression of cyclin B1 was determined by western blotting and real-time PCR. Data are presented as the mean  $\pm$  SEM. \*\*  $P < 0.01$ . (E, F) After downregulation of miR-137, expression of cyclin B1 was determined by western blotting and real-time PCR. Data are presented as the mean  $\pm$  SEM. \*\*  $P < 0.01$ .



*miR-137 inhibits the proliferation of hypertrophic scar fibroblasts by suppressing cyclin B1*

The proliferation of hypertrophic scar fibroblasts was measured using the MTT assay after transfection of miR-637 mimic or inhibitor into fibroblasts. We found that miR-137 mimic could inhibit proliferation of hypertrophic scar fibroblasts and miR-137 inhibitor could promote the proliferation of hypertrophic scar fibroblasts (Fig. 3A, B). Studies have shown that PTN can affect the cell cycle-related protein cyclin B1 by regulating the signaling pathway. Thus, the expression of cyclin B1 in hypertrophic scar fibroblasts with overexpression or underexpression of miR-137 was detected by western blotting and real-time PCR. The results showed that miR-137 could significantly inhibit the expression of cyclin B1 (Fig. 3C-F).

**Fig. 4.** miR-137 inhibits metastasis of hypertrophic scar fibroblasts by suppressing MMP9. (A, B) After overexpression of miR-137 in hypertrophic scar fibroblasts, transwell assay with or without Matrigel was performed. Cells were counted and results represent the mean  $\pm$  standard deviation (SD) of 3 experiments. \*\* P<0.01. (C, D) After downregulation of miR-137 in hypertrophic scar fibroblasts, transwell assay with or without Matrigel was performed. Cells were counted and results represent the mean  $\pm$  SD of 3 experiments. \*\* P<0.01. (E, F) After transfection with miR-137 mimic in hypertrophic scar fibroblasts, the expression of MMP9 were determined by western blotting and real-time PCR. Data are presented as the mean  $\pm$  SEM. \*\* P<0.01. (G, H) After downregulation of miR-137, the expression of MMP9



was determined by western blotting and real-time PCR. Data are presented as the mean  $\pm$  SEM. \*\* P<0.01.

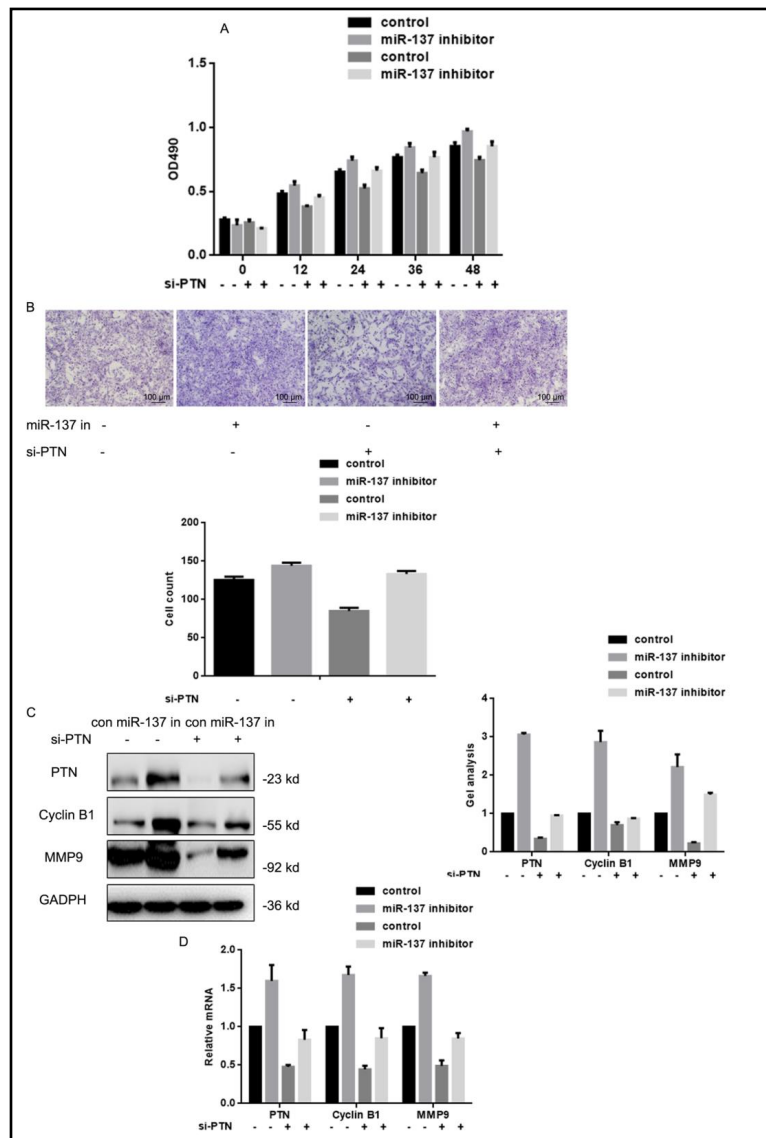
*miR-137 inhibits the metastasis of hypertrophic scar fibroblasts by suppressing MMP9*

High expression of PTN has been shown to affect cell metastasis by regulating MMPs [14]. The transwell assay (with or without Matrigel) was used to study the role of miR-137 in metastasis of hypertrophic scar fibroblasts (Fig. 4A-D). We found that both migration and invasion of hypertrophic scar fibroblasts could be significantly inhibited by miR-137. In addition, western blotting and real-time PCR showed that MMP9 was significantly downregulated by miR-137 (Fig. 4E-H).

*Effects of miR-137 small interfering RNA and PTN siRNA on cell proliferation and metastasis in hypertrophic scar fibroblasts*

We explored the effects of miR-137 small interfering RNA (siRNA) and PTN siRNA on cell proliferation and metastasis in hypertrophic scar fibroblasts. MTT and transwell assays showed that PTN siRNA significantly suppressed cell proliferation and metastasis (Fig. 5A, B). When both miR-137 and PTN were inhibited, proliferation and migration of the cells were reduced compared with the use of miR-137 alone, but proliferation and migration were increased compared with the use of si-PTN alone. In order to explore the underlying molecular mechanisms, cyclin B1 and MMP9 expression levels were determined. Co-

**Fig. 5.** Effects of miR-137 siRNA and PTN siRNA on cell proliferation and metastasis of hypertrophic scar fibroblasts. (A) Effects of miR-137 siRNA and PTN siRNA on cell proliferation were determined using the MTT assay. Data are presented as the mean ± SEM. (B) Effects of miR-137 siRNA and PTN siRNA on cell proliferation were determined using the transwell assay. Cells were counted and results represent the mean ± SD of 3 experiments. (C, D) Effects of miR-137 siRNA and PTN siRNA on PTN, cyclin B1, and MMP9 were determined by western blotting and real-time PCR.



treatment with PTN siRNA and miR-137 inhibitor significantly downregulated the level of PTN compared with cells treated with miR-137 inhibitor alone, the same as the expression level of cyclin B1 and MMP9 (Fig. 5C, D). These results suggest that miR-137 may regulate the proliferation and metastasis of hypertrophic scar fibroblasts by targeting PTN.

## Discussion

Results demonstrated that miR-21 can promote the occurrence and development of hypertrophic scars through regulation of human telomerase reverse transcriptase via phosphatase and tensin homolog [15]. miR-98 inhibits cell proliferation via targeting Col1A1 in human hypertrophic scar fibroblasts [16], and miR-181b may be a potential therapy for hypertrophic scar [17]. Furthermore, miR-137 was decreased in several cancers, and a low miR-137 level was an independent risk factor for cancer [18-22]. MiR-137 could promote the recovery of spinal cord injury [23, 24]. *In vivo* and *in vitro* experiments showed that miR-137 inhibited tumor growth and promoted recovery of injury. Thus, we believe that the biological safety of miR-137 has been demonstrated. However, the role and molecular mechanism of miR-137 and PTN in hypertrophic scars remain unclear.

PTN has mitogenic effects on epithelial cells, endothelial cells, and fibroblasts [8]. Cell proliferation can be promoted by the regulated function of PTN on cell cycle-related proteins (e.g. cyclins D1 and B1). The results from this study showed that high PTN expression significantly correlates with cell metastasis. It has been reported that PTN is overexpressed in hypertrophic scars [8], but the specific underlying mechanisms remain unclear.

In this study, miRNA expression profiling was performed and a unique miRNA signature associated with hypertrophic scar development was identified. Ten miRNAs (miR-137, miR-627-3p, miR-219b-5p, miR-96-3p, miR-548c-3p, miR-384, miR-670-3p, miR-5691, miR-3193-3p, and miR-6805-3p) were found to have a lower expression in hypertrophic scars, and 8 miRNAs (miR-5692b, miR-190a-3p, miR-513a-3p, miR-1279, miR-514b-3p, miR-19a-3p, miR-29b-3p, and miR-3974) were upregulated in hypertrophic scars. The majority of these miRNAs have been reported to function as oncogenes or tumor suppressors, which supports the assumption of similar excess proliferation in hypertrophic scars and cancer cells [25]. Our analysis showed that miR-137 was significantly downregulated in hypertrophic scar tissues. Real-time PCR also confirmed that miR-137 decreased by nearly two-thirds compared with normal tissues. Here, we demonstrated that miR-137 regulated PTN expression by directly targeting the PTN 3'-UTR. We also demonstrated that transfection of fibroblasts with an miR-137 mimic decreased the expression of PTN, while inhibition of miR-137 enhanced PTN expression. Furthermore, we found that miR-137 could inhibit fibroblast differentiation, as demonstrated by reduced expression of  $\alpha$ -SMA, vimentin, and COL1A. Moreover, miR-137 significantly inhibited the proliferation and metastasis of fibroblasts, as shown by the results of the MTT and transwell assays. The expression levels of cyclin B1 and MMP9 could be inhibited by the miR-137 mimic. This suggests that fibroblast proliferation and metastasis were promoted by PTN activation and that this effect was mediated by decreased PTN expression resulting from overexpression of miR-137. Although further *in vivo* experiments are needed to verify our results, we have demonstrated that inhibition of miR-137 expression allows promotion of proliferation and metastasis of fibroblasts.

## Conclusion

The results of this study suggest that miR-137 is a suppressor that exerts its effect through regulation of PTN signaling in hypertrophic scars and provides a potential target for therapy.

## Disclosure Statement

The authors declare no conflict of interests.

## References

- 1 Diegidio P, Hermiz S, Hibbard J, Kosorok M, Hultman CS: Hypertrophic burn scar research: From quantitative assessment to designing clinical sequential multiple assignment randomized trials. *Clin Plast Surg* 2017;44:917-924.
- 2 Li J, Chen L, Cao C, Yan H, Zhou B, Gao Y, Li Q, Li J: The long non-coding rna lncrna8975-1 is upregulated in hypertrophic scar fibroblasts and controls collagen expression. *Cell Physiol Biochem* 2016;40:326-334.
- 3 Friedrich EE, Niknam-Bienia S, Xie P, Jia SX, Hong SJ, Mustoe TA, Galiano RD: Thermal injury model in the rabbit ear with quantifiable burn progression and hypertrophic scar. *Wound Repair Regen* 2017;25:327-337.
- 4 Mohammadi AA, Eskandari S, Johari HG, Rajabnejad A: Using amniotic membrane as a novel method to reduce post-burn hypertrophic scar formation: A prospective follow-up study. *J Cutan Aesthet Surg* 2017;10:13-17.
- 5 Dong S, Sun Y: MircoRNA-22 may promote apoptosis and inhibit the proliferation of hypertrophic scar fibroblasts by regulating the mitogen-activated protein kinase/extracellular signal-regulated kinase/p21 pathway. *Exp Ther Med* 2017;14:3841-3845.
- 6 Wang WH, Deng AJ, He SG: A key role of mircoRNA-26a in the scar formation after glaucoma filtration surgery. *Artif Cells Nanomed Biotechnol* 2017:1-7.
- 7 Li G, Zhou R, Zhang Q, Jiang B, Wu Q, Wang C: Fibroproliferative effect of mircoRNA-21 in hypertrophic scar derived fibroblasts. *Exp Cell Res* 2016;345:93-99.
- 8 Zhang Q, Tao K, Huang W, Tian Y, Liu X: Elevated expression of pleiotrophin in human hypertrophic scars. *J Mol Histol* 2013;44:91-96.
- 9 Gras C, Ratuszny D, Hadamitzky C, Zhang H, Blasczyk R, Figueiredo C: MiR-145 contributes to hypertrophic scarring of the skin by inducing myofibroblast activity. *Mol Med* 2015;21:296-304.
- 10 Feng J, Wang K, Liu X, Chen S, Chen J: The quantification of tomato mircoRNAs response to viral infection by stem-loop real-time rt-pcr. *Gene* 2009;437:14-21.
- 11 Chen C, Ridzon DA, Broomer AJ, Zhou Z, Lee DH, Nguyen JT, Barbisin M, Xu NL, Mahuvakar VR, Andersen MR, Lao KQ, Livak KJ, Guegler KJ: Real-time quantification of mircoRNAs by stem-loop rt-pcr. *Nucleic Acids Res* 2005;33:e179.
- 12 Pfaffl MW: A new mathematical model for relative quantification in real-time rt-pcr. *Nucleic Acids Res* 2001;29:e45.
- 13 Yang TS, Yang XH, Wang XD, Wang YL, Zhou B, Song ZS: MiR-214 regulate gastric cancer cell proliferation, migration and invasion by targeting pten. *Cancer Cell Int* 2013;13:68.
- 14 Zha L, He L, Xie W, Cheng J, Li T, Mohsen MO, Lei F, Storni F, Bachmann M, Chen H, Zhang Y: Therapeutic silence of pleiotrophin by targeted delivery of sirna and its effect on the inhibition of tumor growth and metastasis. *PLoS One* 2017;12:e0177964.
- 15 Zhu HY, Li C, Bai WD, Su LL, Liu JQ, Li Y, Shi JH, Cai WX, Bai XZ, Jia YH, Zhao B, Wu X, Li J, Hu DH: MircoRNA-21 regulates htert via pten in hypertrophic scar fibroblasts. *PLoS One* 2014;9:e97114.
- 16 Zhang JJ, Chen JT, Hua L, Yao KH, Wang CY: MiR-98 inhibits hepatocellular carcinoma cell proliferation via targeting ezh2 and suppressing wnt/beta-catenin signaling pathway. *Biomed Pharmacother* 2017;85:472-478.
- 17 Kwan P, Ding J, Tredget EE: MircoRNA 181b regulates decorin production by dermal fibroblasts and may be a potential therapy for hypertrophic scar. *PLoS One* 2015;10:e0123054.
- 18 Bi Y, Han Y, Bi H, Gao F, Wang X: MiR-137 impairs the proliferative and migratory capacity of human non-small cell lung cancer cells by targeting paxillin. *Hum Cell* 2014;27:95-102.
- 19 Chen R, Zhang Y, Zhang C, Wu H, Yang S: MiR-137 inhibits the proliferation of human non-small cell lung cancer cells by targeting src3. *Oncol Lett* 2017;13:3905-3911.

- 20 Deng J, Lei W, Xiang X, Zhang L, Lei J, Gong Y, Song M, Wang Y, Fang Z, Yu F, Feng M, Sun Z, Chen J, Zhan Z, Xiong J: Cullin 4a (cul4a), a direct target of miR-9 and miR-137, promotes gastric cancer proliferation and invasion by regulating the hippo signaling pathway. *Oncotarget* 2016;7:10037-10050.
- 21 Dong P, Xiong Y, Watari H, Hanley SJ, Konno Y, Ihira K, Yamada T, Kudo M, Yue J, Sakuragi N: MiR-137 and miR-34a directly target snail and inhibit emt, invasion and sphere-forming ability of ovarian cancer cells. *J Exp Clin Cancer Res : CR* 2016;35:132.
- 22 Du Y, Chen Y, Wang F, Gu L: MiR-137 plays tumor suppressor roles in gastric cancer cell lines by targeting klf12 and myo1c. *Tumour Biol* 2016;37:13557-13569.
- 23 Dai J, Xu LJ, Han GD, Sun HL, Zhu GT, Jiang HT, Yu GY, Tang XM: MiR-137 attenuates spinal cord injury by modulating neurod4 through reducing inflammation and oxidative stress. *Eur Rev Med Pharmacol Sci* 2018;22:1884-1890.
- 24 Li J, Li J, Wei T, Li J: Down-regulation of mircoRNA-137 improves high glucose-induced oxidative stress injury in human umbilical vein endothelial cells by up-regulation of ampkalpha1. *Cell Physiol Biochem* 2016;39:847-859.
- 25 Guo L, Xu K, Yan H, Feng H, Wang T, Chai L, Xu G: MircoRNA expression signature and the therapeutic effect of the mircoRNA21 antagomir in hypertrophic scarring. *Mol Med Rep* 2017;15:1211-1221.